

Report

**P-20-15**

July 2020



# Task 9B – A grain-scale reactive transport model – concepts and tests

Task 9 of SKB Task Force GWFTS – Increasing the realism in solute transport modelling based on the field experiments REPRO and LTDE-SD

Urban Svensson

SVENSK KÄRNBRÄNSLEHANTERING AB

SWEDISH NUCLEAR FUEL  
AND WASTE MANAGEMENT CO

Box 3091, SE-169 03 Solna  
Phone +46 8 459 84 00  
skb.se

SVENSK KÄRNBRÄNSLEHANTERING



ISSN 1651-4416

**SKB P-20-15**

ID 1896515

July 2020

## **Task 9B – A grain-scale reactive transport model – concepts and tests**

### **Task 9 of SKB Task Force GWFTS – Increasing the realism in solute transport modelling based on the field experiments REPRO and LTDE-SD**

Urban Svensson

Computer-aided Fluid Engineering AB

*Keywords:* Reactive transport, Numerical model, Particle tracking, LTDE-SD.

This report concerns a study which was conducted for Svensk Kärnbränslehantering AB (SKB). The conclusions and viewpoints presented in the report are those of the author. SKB may draw modified conclusions, based on additional literature sources and/or expert opinions.

Data in SKB's database can be changed for different reasons. Minor changes in SKB's database will not necessarily result in a revised report. Data revisions may also be presented as supplements, available at [www.skb.se](http://www.skb.se).

A pdf version of this document can be downloaded from [www.skb.se](http://www.skb.se).

© 2020 Svensk Kärnbränslehantering AB



## Preface

The work described in this report was carried out during 2016–2017 and reported as a Technical Note 2017-06-30. Several years have thus passed before the project now is documented as a SKB report. One reason for this Preface is therefore to connect this work to what followed. Another reason is to point out some important developments that subsequently have proved to be of interest.

Let us start by listing some important developments achieved in the Task 9B project:

- A synthetic grain block was developed. A certain percentage of the grains was prescribed as reactive. This was a useful step before X-ray micro computed tomography data was introduced.
- A reactive transport model based on particle tracking was introduced. Based on the concept “when a particle is close to a reactive grain it has a certain probability to get sorbed during a certain time span. Once sorbed it will stay so a certain time”, this model has proved to be a useful tool.
- Quartz veins. The experimental data suggested “deep penetration into the rock matrix”. One way to achieve this in the models is to introduce deterministic fractures and assume that these go through quartz grains (quartz grains are not reactive). Experimental data for the fractures were available.
- Computational methods. A grid that resolved the intergranular space was developed; cells inside grains could be removed, which reduced the number of cells significantly. For particle tracking the CTRW (Continuous Time Random Walk) method was included as an option in DarcyTools.

These are the developments that are regarded as most significant and proved to be “building blocks” for coming projects.

It is clear that Task 9B initiated several ideas and methods that were further developed in Task 9C. Results from Task 9C have been reported in form of three published papers. Abstract from these are included in this Preface as they show the link to the early steps carried out in Task 9B.

**Svensson U, Löfgren M, Trinchero P, Selroos J-O, 2018.** Modelling the diffusion-available pore space of an unaltered granitic rock matrix using a micro-DFN approach. *Journal of Hydrology* 559, 182–191.

In sparsely fractured rock, the ubiquitous heterogeneity of the matrix, which has been observed in different laboratory and in situ experiments, has been shown to have a significant influence on retardation mechanisms that are of importance for the safety of deep geological repositories for nuclear waste. Here, we propose a conceptualisation of a typical heterogeneous granitic rock matrix based on micro-Discrete Fracture Networks (micro-DFN). Different sets of fractures are used to represent grain-boundary pores as well as micro fractures that transect different mineral grains. The micro-DFN model offers a great flexibility in the way inter- and intra-granular space is represented as the different parameters that characterise each fracture set can be fine tuned to represent samples of different characteristics. Here, the parameters of the model have been calibrated against experimental observations from granitic rock samples taken at Forsmark (Sweden) and different variant cases have been used to illustrate how the model can be tied to rock samples with different attributes. Numerical through-diffusion simulations have been carried out to infer the bulk properties of the model as well as to compare the computed mass flux with the experimental data from an analogous laboratory experiment. The general good agreement between the model results and the experimental observations shows that the model presented here is a reliable tool for the understanding of retardation mechanisms occurring at the mm-scale in the matrix.

**Svensson U, Voutilainen M, Muuri E, Ferry M, Gylling B, 2019.** Modelling transport of reactive tracers in a heterogeneous crystalline rock matrix. *Journal of Contaminant Hydrology* 227. <https://doi.org/10.1016/j.jconhyd.2019.103552>.

A numerical reactive transport model for crystalline rocks is developed and evaluated. The model is based on mineral maps generated by X-ray micro computed tomography (X- $\mu$ CT); these maps have a resolution of approximately 10  $\mu$ m and the rock samples are on the cm scale. A computational

grid for the intergranular space is generated and a micro-DFN (Discrete Fracture Network) model governs the grid properties. A particle tracking method (Time Domain Random Walk) is used for transport simulations. The basic concept of the model can now be stated as follows; “when a particle is close to a reactive mineral surface it has a certain probability to get sorbed during a certain time span. If sorbed it will stay so a certain time”. The model requires a number of input parameters. Attempts are made to relate these to traditional distribution parameters. The model is evaluated by comparisons with recent experimental data from laboratory experiments. These experiments consider two rock types (veined gneiss and pegmatitic granite) and two radionuclides (cesium and barium). It is concluded that the new reactive transport model can simulate the experimental data in a consistent and realistic way.

**Svensson U, Trinchero P, Ferry M, Voutilainen M, Gylling B, Selroos J-O, 2019.** Grains, grids and mineral surfaces: approaches to grain scale matrix modelling based on X-ray micro-computed tomography data. *SN Applied Sciences* 1, 1277. <https://doi.org/10.1007/s42452-019-1254-1>.

X-ray micro-computed tomography (X- $\mu$ CT) generates 3D mineral distribution maps currently with a resolution of about 10  $\mu$ m. For tight crystalline rocks, this implies that the mineral grains are well resolved, while micro-fractures, having apertures of less than 10  $\mu$ m, are not resolved. In this study, we propose a method to analyze the properties (size, volume, surface area) of the mineral grains based on X- $\mu$ CT data. The numerical approach uses a resolution similar to that of the X- $\mu$ CT data and hence shares the same limitations. For example, it is clear that a large fraction of the mineral surface area is due to so-called roughness, with scales below 10  $\mu$ m. In the second part of the study, methods to generate the diffusion-available pore space are discussed. The inter-granular space (distance between grains) is often smaller than 10  $\mu$ m, and we need to design methods to be able to perform diffusion simulations in the matrix. Three methods, all based on X- $\mu$ CT, are discussed, and it is demonstrated that models with realistic global properties (mean porosity and effective diffusion coefficient) can be developed based on the suggested techniques.

## **Abstract**

The development of a reactive particle tracking model is initiated. The basic concept of the model is “when a particle is close to a reactive grain it has a certain probability to get sorbed during a certain time span. Once sorbed it will stay so a certain time”. Attempts are made to relate the model parameters to more traditional retention parameters. An overall objective of the project is to simulate the LTDE-SD experiment. Results from this application are presented. The main conclusion from the project is that a promising development of a reactive particle tracking method has been initiated.

## Sammanfattning

Utvecklingen av en reaktiv partikelmodell har initierats. Den grundläggande idén är ”en partikel som befinner sig nära en reaktiv kornyta har en viss sannolikhet att absorberas under ett visst tidsintervall. Om den absorberas så förblir den så en viss tid”. Genom att testa modellen på renodlade geometrier och förutsättning, så kan modellens parametrar relateras till mer traditionella retentionsparametrar. Ett övergripande syfte med projektet är att simulera resultat från LTDE-SD experimentet. Resultat från denna applicering av modellen presenteras och diskuteras. Det viktigaste resultatet av arbetet är att utvecklingen av en reaktiv partikelmodell har initierats.



# Contents

<b>1</b>	<b>Introduction</b>	9
1.1	Background	9
1.2	LTDE	9
1.3	Matrix Model	9
1.4	Objective	9
<b>2</b>	<b>Conceptual model</b>	11
2.1	The DarcyTools Matrix Model	11
2.2	Generic LTDE	11
2.3	Known Fractures	11
2.4	Methods	12
<b>3</b>	<b>Results</b>	15
3.1	1D tests of methods	15
3.2	$K_d$ experiments	15
3.3	3D Through-Diffusion	20
3.4	LTDE, generic	22
3.5	LTDE, the stub	28
<b>4</b>	<b>Discussion</b>	35
4.1	Experimental data	35
4.2	Basic knowledge	35
4.3	The model	35
<b>5</b>	<b>Summary and conclusions</b>	37
	<b>References</b>	39



# 1 Introduction

## 1.1 Background

Transport of radionuclides through a granitic rock matrix is, for obvious reasons, of interest to SKB. Transport is due to advection and/or diffusion; if no large flowing fracture is present, one can normally assume that diffusion dominates the transport. If the radionuclide reacts with individual grains, the transport process may be significantly slowed down. In this study a numerical model of transport and reactions will be evaluated. A general description of Task 9B is given by the Task description (Löfgren and Nilsson 2020).

## 1.2 LTDE

Three reports (Widestrand et al. 2010a, b, Nilsson et al. 2010) give a full account of the LTDE-SD experiment. Here, only a brief introduction, see Figure 1-1, is given. In a fracture, called the target fracture, a cocktail of radionuclides is circulated for a period of about 200 days. After this time cores are drilled and the penetration of the radionuclides is analysed. The profiles, from the target fracture inwards, are one of the key results of the experiment.

## 1.3 Matrix Model

Within the framework of the code DarcyTools (Svensson and Ferry 2014) a matrix model has been developed. In three recent papers (Svensson et al. 2018, Svensson et al. 2019a,b) this model has been documented, tested and applied. The work carried out in Task 9B, can be considered as the initiation of the development of the matrix model.

## 1.4 Objective

Initiate a development of a reactive transport model for a granitic rock matrix.

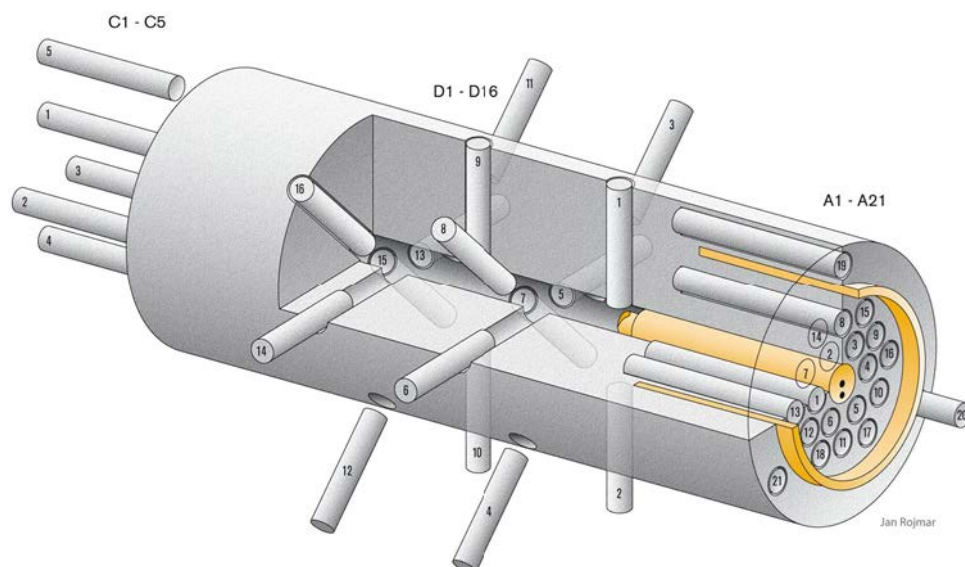


**Figure 1-1.** Illustration of drill core samples drilled from the over-cored rock volume. The A-core samples are drilled from the target fracture and the D-core samples correspond to the slim hole.



## 2 Conceptual model

### 2.1 The DarcyTools Matrix Model

As mentioned above, the matrix model has recently been documented; we can hence be brief in this context. The basic feature is illustrated in Figure 2-1. Three fracture sets are generated: one set can be called a “traditional DFN” as it concerns fractures larger than the grain size. The set with a length interval 4–5 mm (depending on the grain size to be simulated) generates a network that defines the intergranular path ways. The micro fracture set,  $l = 1\text{--}2$  mm, is needed to provide the complexity of the intergranular volumes (dead ends, multiple pathways, etc.).

### 2.2 Generic LTDE

The LTDE-SD experiment was introduced in Figure 1-1. In Figure 2-2 a generic version is given, which is intended to show the basic concepts of the diffusion process (advection can be neglected). A radionuclide that diffuses into the matrix may get in contact with reactive grains.

When a particle is close to a reactive surface it has a certain probability,  $P_s$ , to get sorbed within a certain time. If sorbed it will stay sorbed for an average time of  $T_s$ .  $P_s$  and  $T_s$  are specified and  $N_{sorb}/N_{free}$  is calculated.  $N_{sorb}$  is the number of particles sorbed and  $N_{free}$  is the number of particles not sorbed. See Figure 2-3. We introduce the parameters  $N_{sorb}$  and  $N_{free}$  already at this stage as these will later be related to  $K_d$ -values.

To set up a numerical model, we hence need to know which radionuclides that will react with a certain grain. This information is generally hard to compile. X-ray tomography may however provide detailed information about the distribution of grains. In this report a synthetic grain distribution is generated.

Let us introduce the grain-block, see Figure 2-4. Three different types are introduced with proportions 60, 30 and 10 %. Introducing three grain types and the given proportions is of course arbitrary at this stage and done only as an illustration. The distribution in space is random. The grain size (size of a small box) is 1.5 mm. The block contains  $35 \times 8 \times 68$  grains and the cube will cover the computational domain to be used for the generic LTDE case (details below). The basic idea is then that every cell centre in the computational grid can pick a grain type from the grain block, simply by comparing the cell centre coordinates with the coordinates in the grain block.

### 2.3 Known Fractures

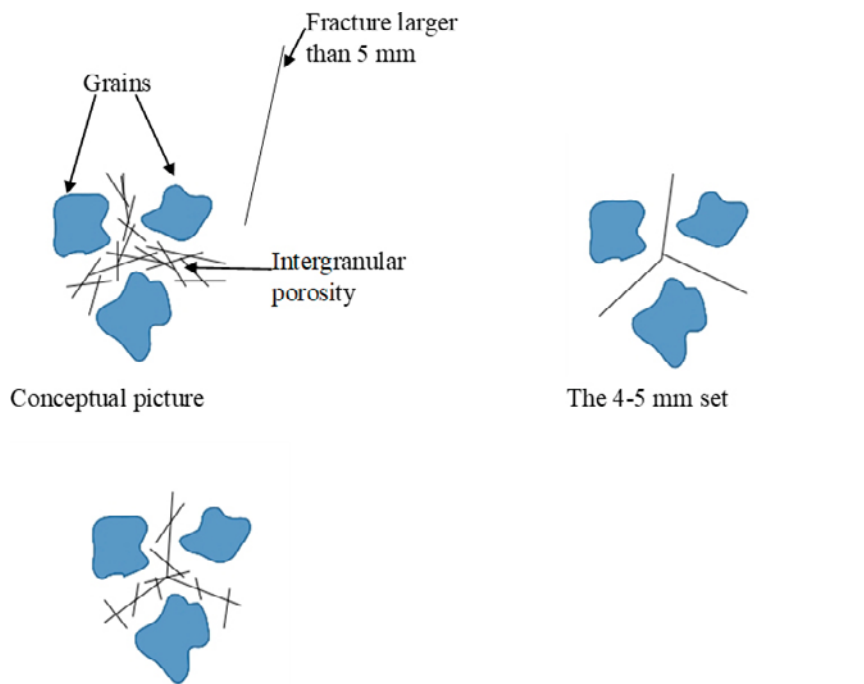
In connection with Figure 2-1, it was said that the set with the largest fractures was a “traditional DFN”. These larger fractures are known to often be located in quartz (quartz veins). As radionuclides do not react with quartz, it is realized that the large fractures may provide fast path ways into the matrix. These are accordingly important for deep penetration of sorbing radionuclides (as they do not sorb on quartz).

One can hence expect that the realism of the model may be improved if the largest fractures were known and could be included in a deterministic way. The experimental team has located the major fractures in the stub, see Figure 2-5, and these will be treated as known fractures. It should be pointed out that it is the geometry that is known, while properties (aperture, diffusion and porosity values, etc.) are presently not available. It is any way regarded as conceptually important to include the known fractures.

## 2.4 Methods

The computational tool to be used is DarcyTools (Svensson and Ferry 2014). DarcyTools embodied a wide range of methods and techniques; in the present context the following features are highlighted:

- Any number of advection/diffusion equations with complex source terms and boundary conditions can be activated.
- A range of particles tracking methods is at hand. In this project we will use the Continuous Time Random Walk (CTRW) method presented by Russian et al. (2015).
- The grid generator has a Remove-Refine-Cells feature. In this project we will use this method to remove cells that are generated in grains, as we do not consider diffusion into grains. This method often removes 70–80 % of the cells in a uniform grid.



A micro fracture set (1-2 mm) is added

**Figure 2-1.** Concepts used in the matrix model.

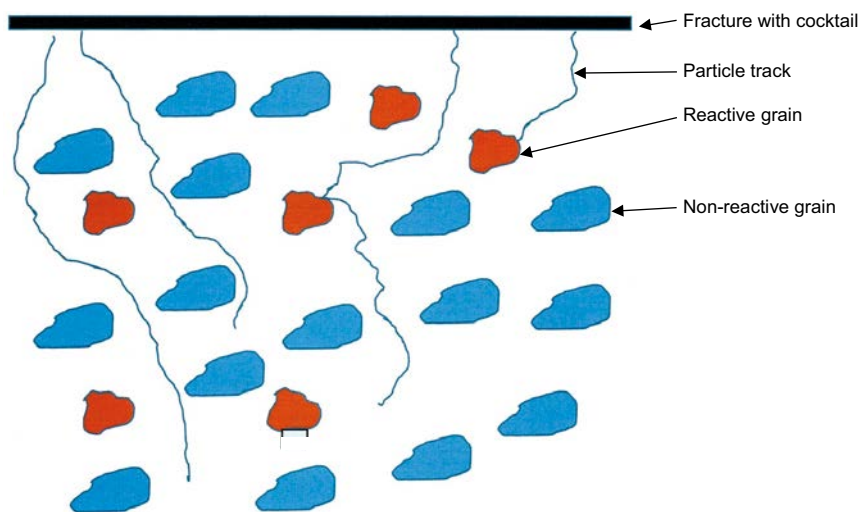


**Figure 2-2.** A generic LTDE sketch. Note that the Brownian motion tracks are much more complex than shown.

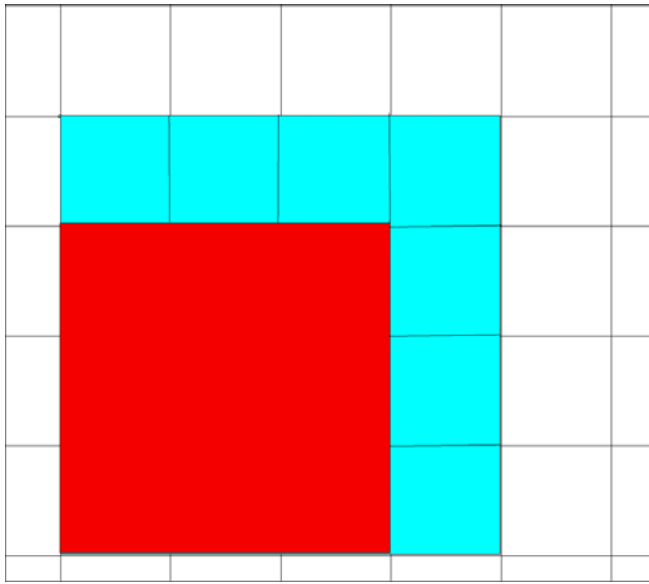


**Figure 2-3.** Illustration of grain cell (red) and grain boundary cells (blue). Particles may get sorbed when in a grain boundary cell.

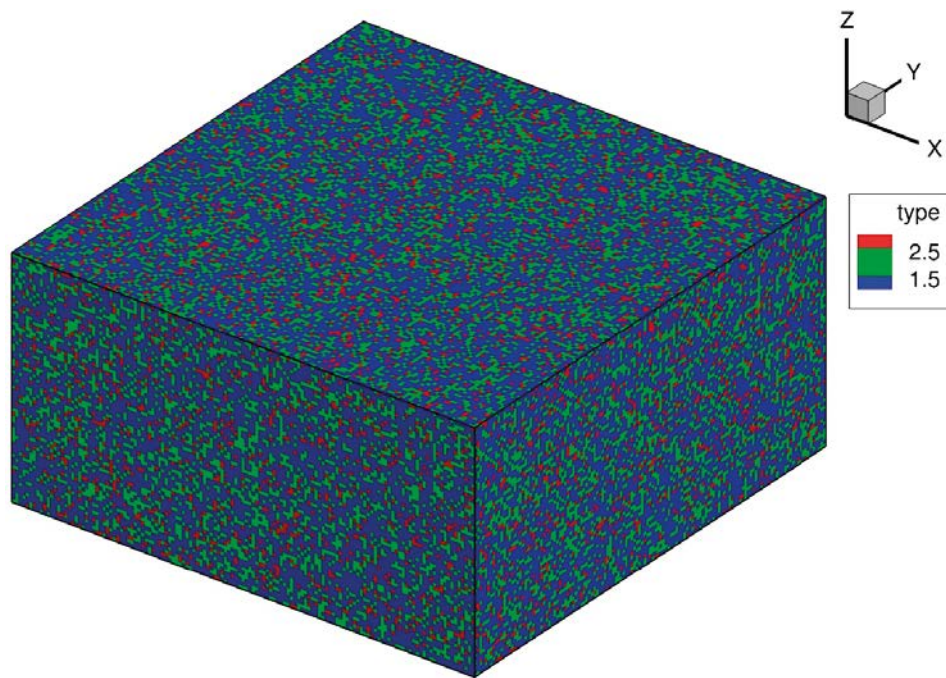


**Figure 2-4.** Grain Block. The block will cover the computational domain used for the LTDE case. Three different grain types (represented by different colours) are generated in specified proportions.

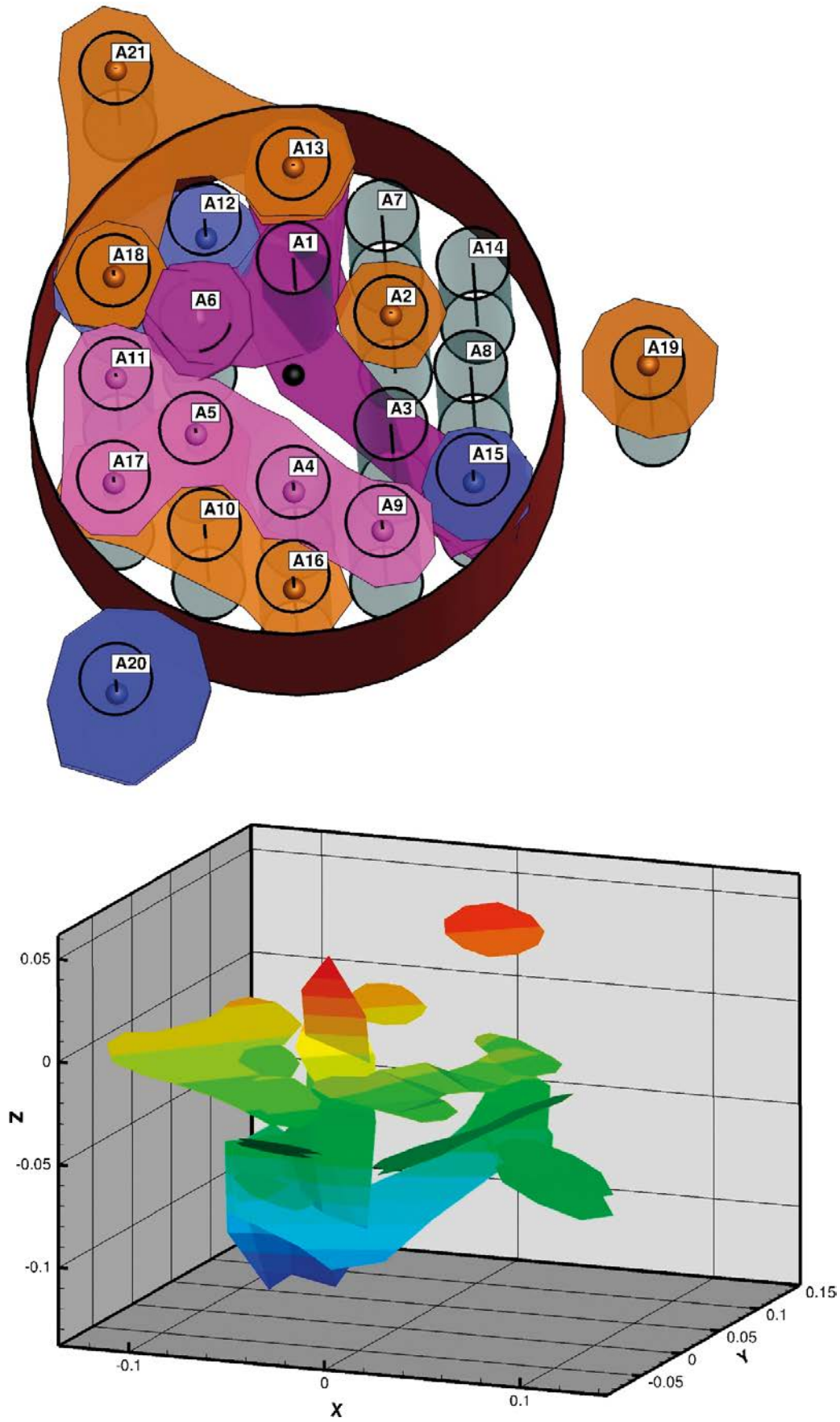


Figure 2-5. Deterministic fractures. With A-cores (top) and coloured with z-coordinate. Coordinates in [m].



## 3 Results

### 3.1 1D tests of methods

The LTDE is an in-diffusion experiment, which in many respects is similar to a through-diffusion experiment. We will use the analytical solution (Crank 1975) for through-diffusion to verify our simulation methods. Both the advection-diffusion (AD) equation and the particle tracking (PTK) method will be verified.

The initial and boundary conditions for the diffusion experiments were as follows:

$$C(x, 0) = 0 \quad x \geq 0$$

$$C(0, t) = C_0 \quad t \geq 0$$

$$C(x, t) = 0 \quad x = d$$

where  $C_0$  is the concentration in the reservoir cell. In accordance with the chosen boundary conditions, the analytical solution of Fick's 2<sup>nd</sup> law for the contaminant mass,  $M$ , that has diffused through the rock slab per unit area is given by (Crank 1975):

$$M = C_0 \alpha d \left( \frac{D_a t}{d^2} - \frac{1}{6} - \frac{2}{\pi^2} \sum_{n=1}^{\infty} \frac{(-1)^n}{n^2} \exp \left[ \frac{-n^2 \pi^2 D_a t}{d^2} \right] \right).$$

Results are shown in Figures 3-1 and 3-2, where also an outline of the situation studied is found. Starting with Figure 3-1, where results for the AD-equation are given, we see that a perfect agreement is found for both porosity values. For the PTK-method, Figure 3-2, a less good agreement is found. This is due to the boundary condition  $C = 1$ ; it is difficult to maintain the exact boundary condition at  $x = 0$ . For the PTK-method there are two options for this boundary; one is to continuously insert particles and the other is to use a "reservoir" with a high density of particles. Here we use the second alternative. A reservoir of a length of 0.02 m will be sufficient for a porosity of 0.1, while a larger one may be needed for a porosity of 1.0. However, it is anyway clear that the analytical solution can be reproduced.

### 3.2 $K_d$ experiments

The objective of this case is to relate the modelling approach to experimentally obtained  $K_d$  values. A cube with side length of 40 mm is used as the computational domain, see Figure 3-3. In this cube a number of grains are placed randomly in space. The grain size is set to 1.5 mm with the intention to simulate experiments with grain size fraction 1–2 mm. To be able to compare simulations with experimental data it is necessary to have the same "liquid to solid ratio" (see Widestrand et al. 2010a, p 28). A ratio of 1 g solid to 4 ml water phase was used. The diffusion coefficient in the water phase was set to  $10^{-9}$  m<sup>2</sup>/s.

At steady state it is noted how many particles are sorbed,  $N_{sorb}$ , and how many are in the water,  $N_{free}$ . The  $K_d$  value can then be calculated as  $K_d = \frac{N_{sorb}}{N_{free}} \times \frac{4 \times 10^{-6}}{10^{-3}}$

where  $4 \times 10^{-6}$  (m<sup>3</sup>) and  $10^{-3}$  (kg) give the liquid to solid ratio.

Simulations for a range of  $P_s$  and  $T_s$  values then results in the diagram shown in Figure 3-4. It is seen that  $K_d$  values from  $10^{-5}$  to 0.1 (m<sup>3</sup>/kg) can be related to  $P_s$  and  $T_s$ . This seems to be a adequate range considering Table 4-11 in Widestrand et al. (2010a).

Illustrations of the particle distribution can be found in Figures 3-5 and 3-6.

It is clear from Figure 3-4 that a certain  $K_d$  value can be specified from different  $P_s$ ; it should then be enough to use one value. Noting that in most cases a cell is in contact with a grain with one out of six cell walls, one could argue that  $P_s$  should be set to 1/6. In some cases two or more cell walls can be in contact which means that a somewhat larger value is motivated. In Figure 3-7 a  $P_s = 0.2$  is used and  $K_d$  values for a range of cell sizes are given. This is useful as the cell size needs to be chosen with respect to the computational domain.

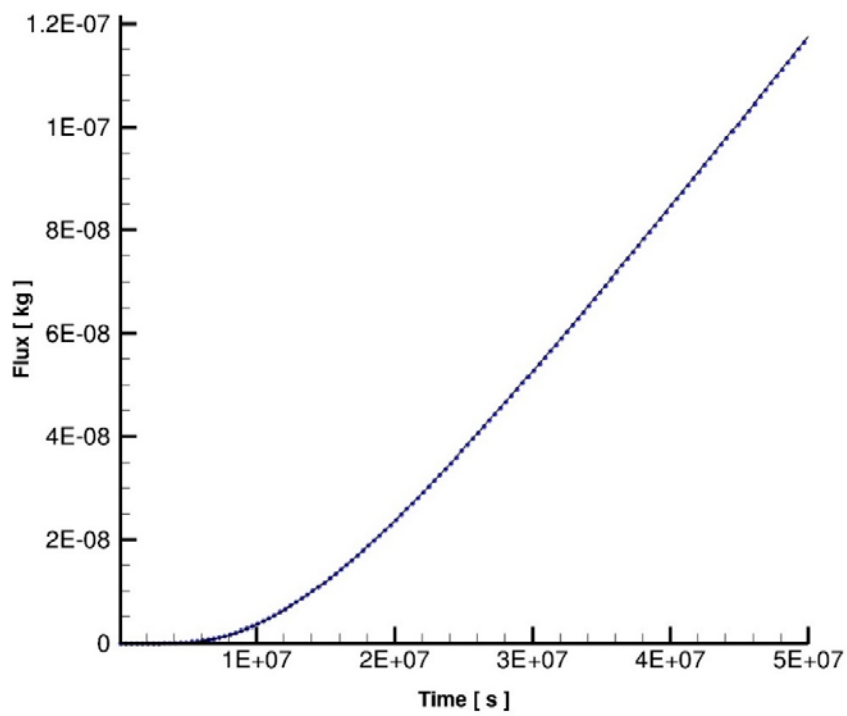
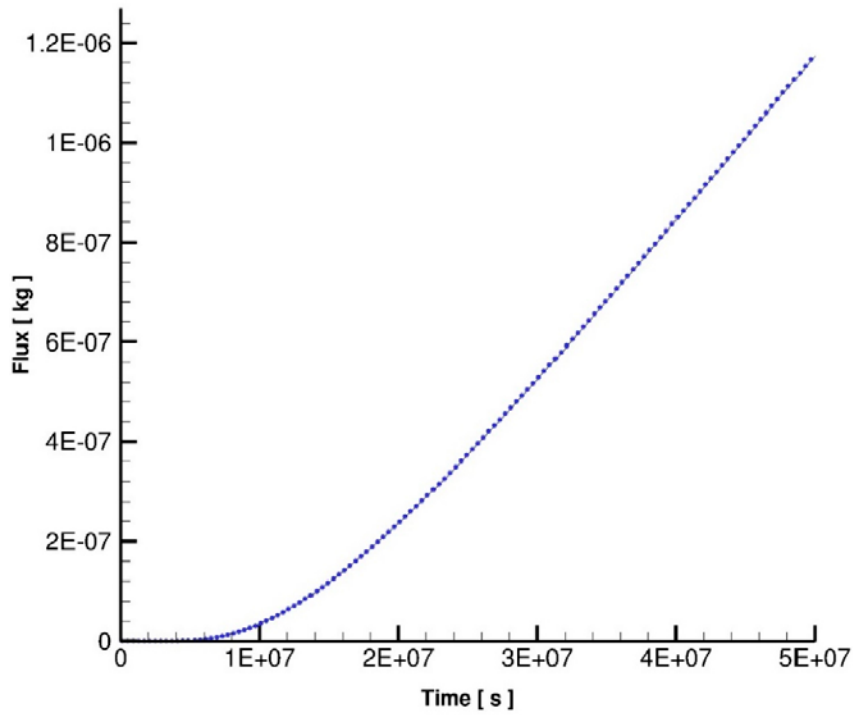
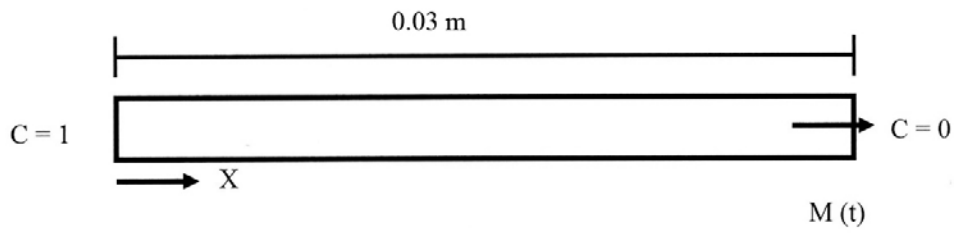


**Figure 3-1.** 1D test. The AD-solution (dots) and the corresponding analytical solution. Porosity equal to 1.0 (top) and 0.1.

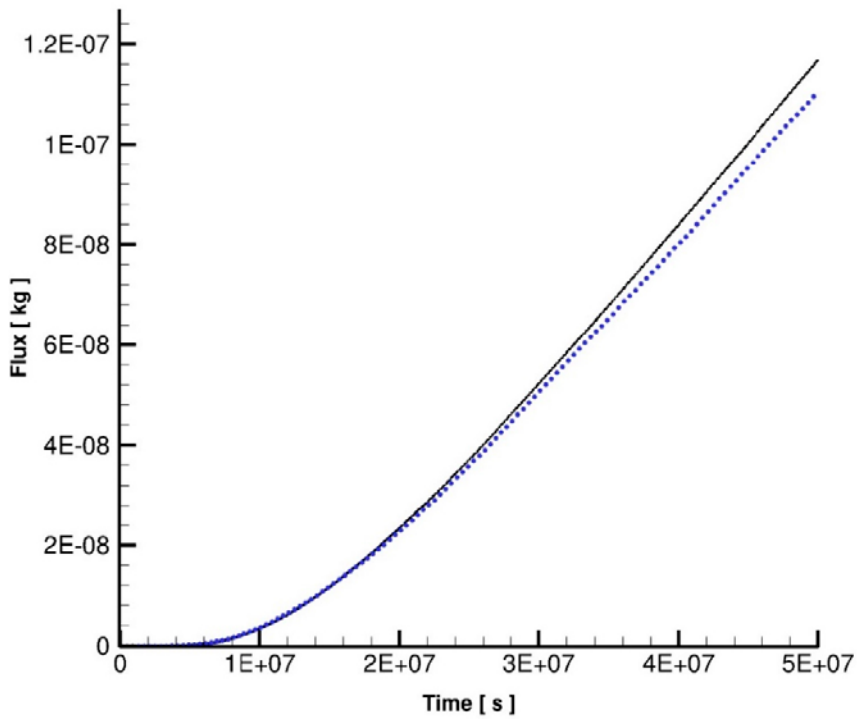
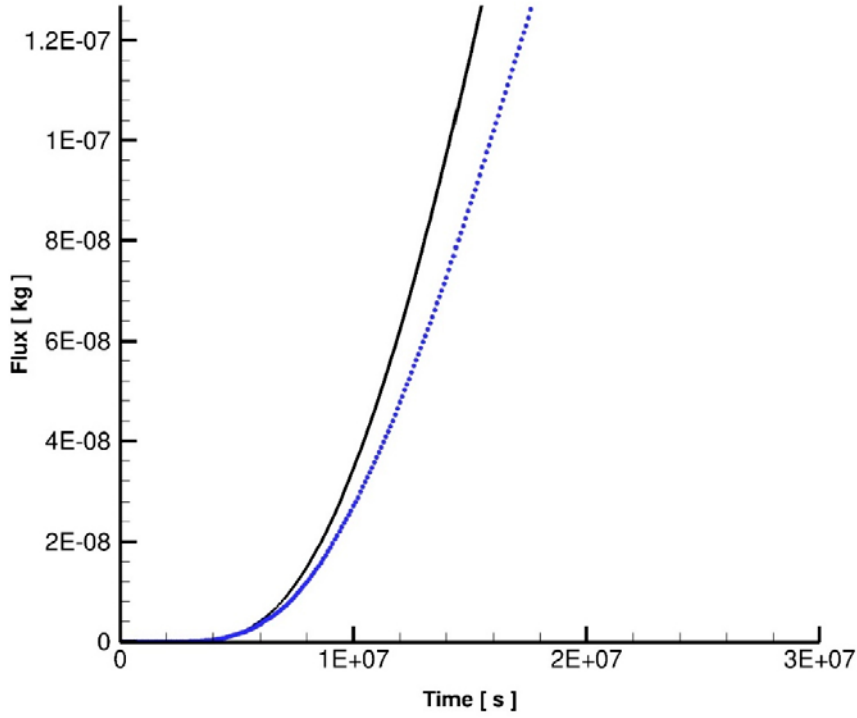
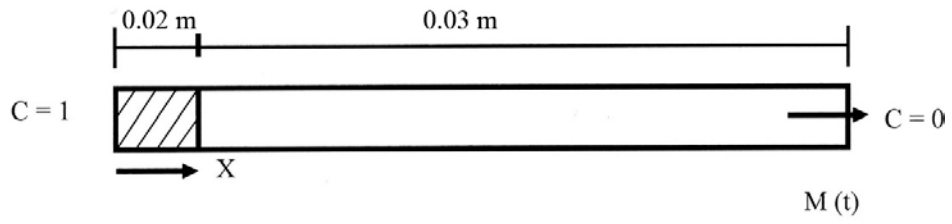


**Figure 3-2.** 1D test. The particle tracking solution (dots) and the corresponding analytical solution. Porosity equal to 1.0 (top) and 0.1.

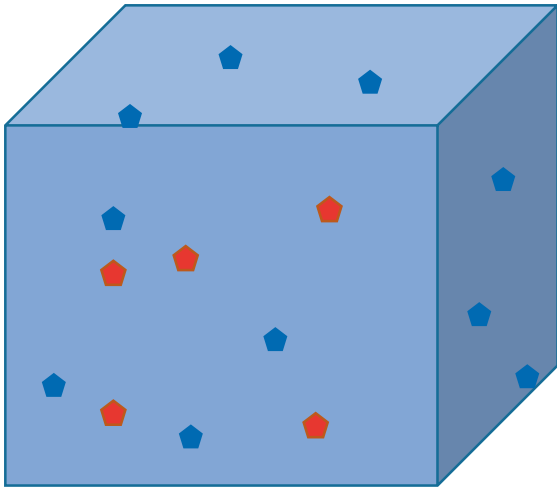


**Figure 3-3.** Steady State Equilibrium case. Computational domain with grains; red grains are reactive.

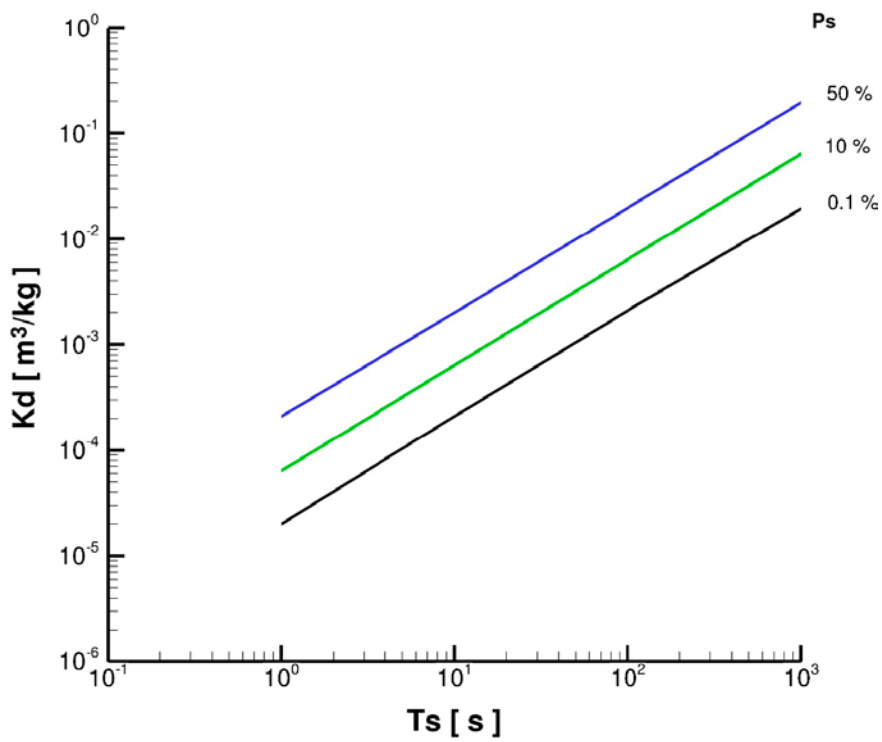


**Figure 3-4.** Steady State Equilibrium case. Relation between  $P_s$ ,  $T_s$  and  $K_d$ .

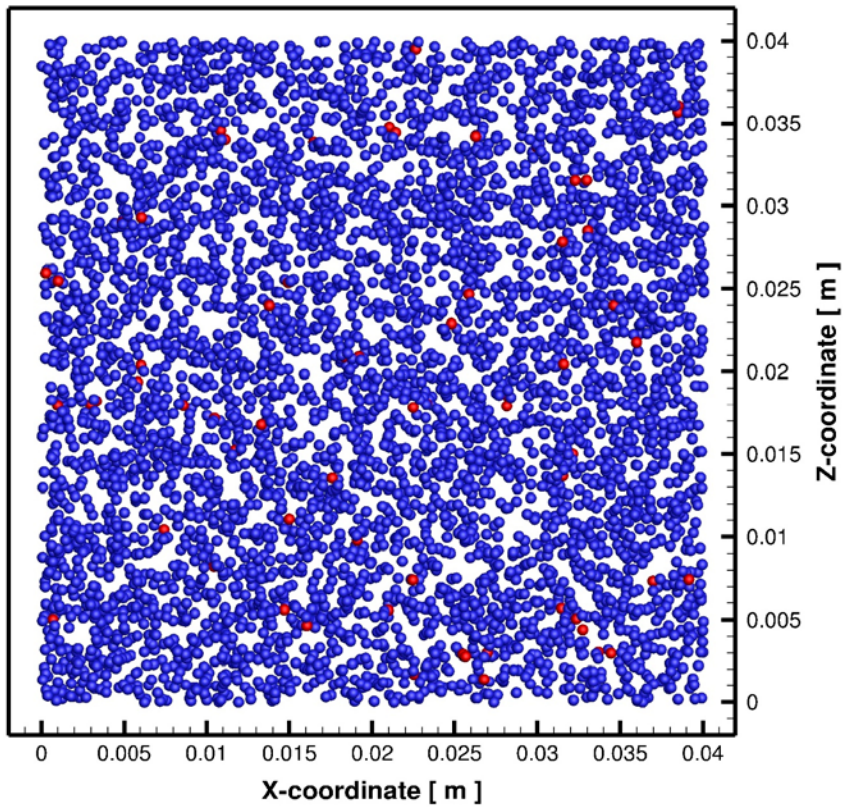


**Figure 3-5.** Steady State Equilibrium case. Particle distribution for  $P_s = 10\%$  and  $T_s = 1$  s. Red particles are sorbed.

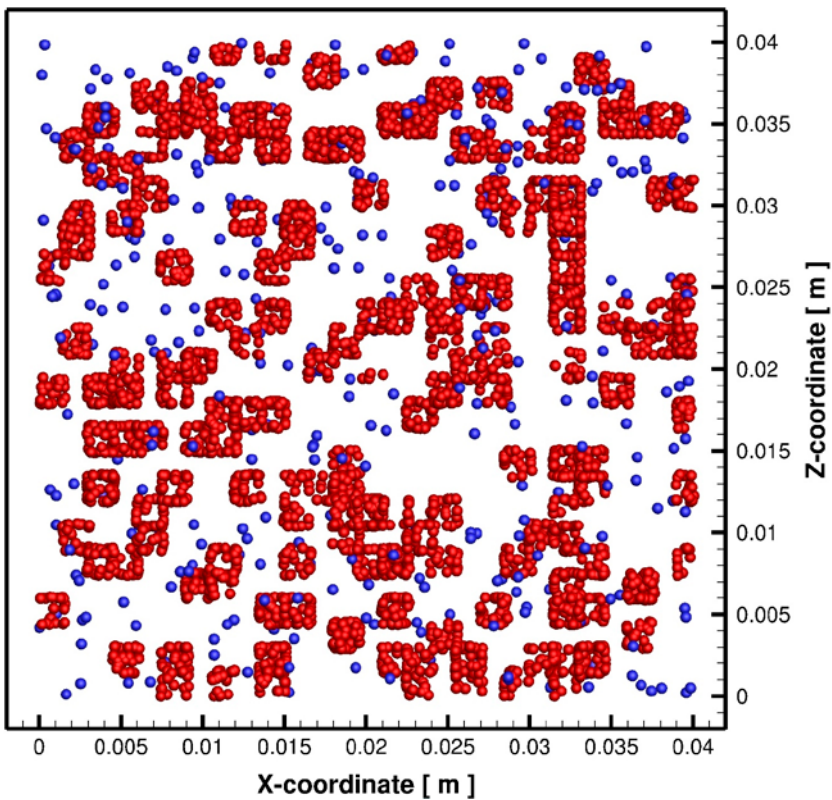


**Figure 3-6.** Steady State Equilibrium case. Particle distribution for  $P_s = 10\%$  and  $T_s = 1000$  s. Red particles are sorbed.

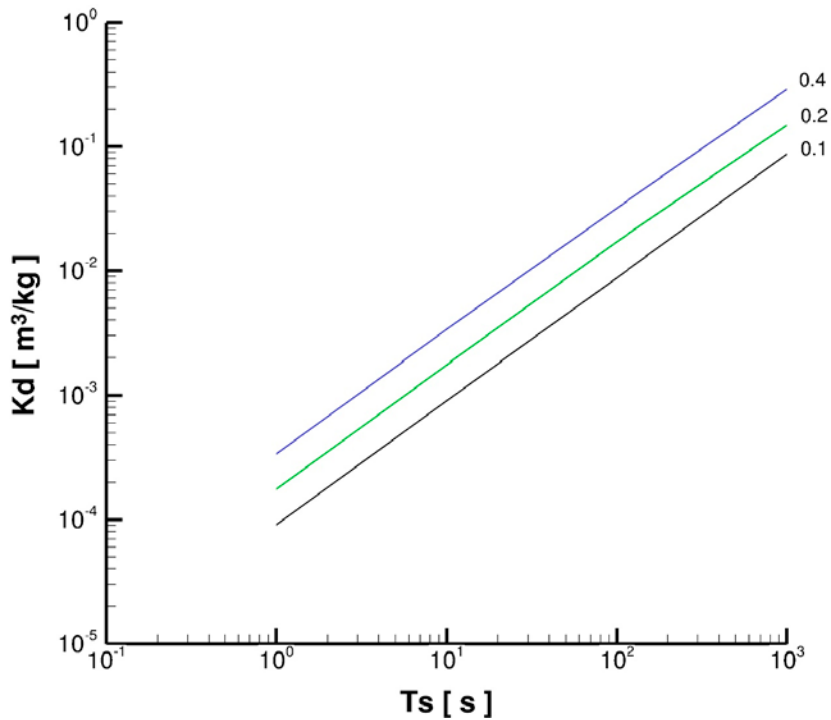


Figure 3-7. Steady state Equilibrium case. Relation between  $T_s$ ,  $K_d$  and cell size (in mm).  $P_s$  fixed to 20 %.

### 3.3 3D Through-Diffusion

Diffusion through a cylindrical sample was studied in order to tune the diffusion coefficient and porosity to experimental data. The cylinder had a diameter of 22 mm and a length of 30 mm and an advection/diffusion equation was solved in order to obtain the steady state tracer distribution. An effective diffusion coefficient is then obtained from the flux through the sample:

$$\text{Flux} = D_e A \frac{dc}{dx}$$

From the simulation  $D_e$  was found to be  $3.5 \times 10^{-13} \text{ m}^2/\text{s}$  and the porosity  $2.2 \times 10^{-3}$ . Some details of the simulation are given in Figure 3-8. The tracer is specified to 1.0 at the low- $z$  boundary and to 0.0 at the high- $z$  boundary. The steady state tracer distribution is shown in Figure 3-8.

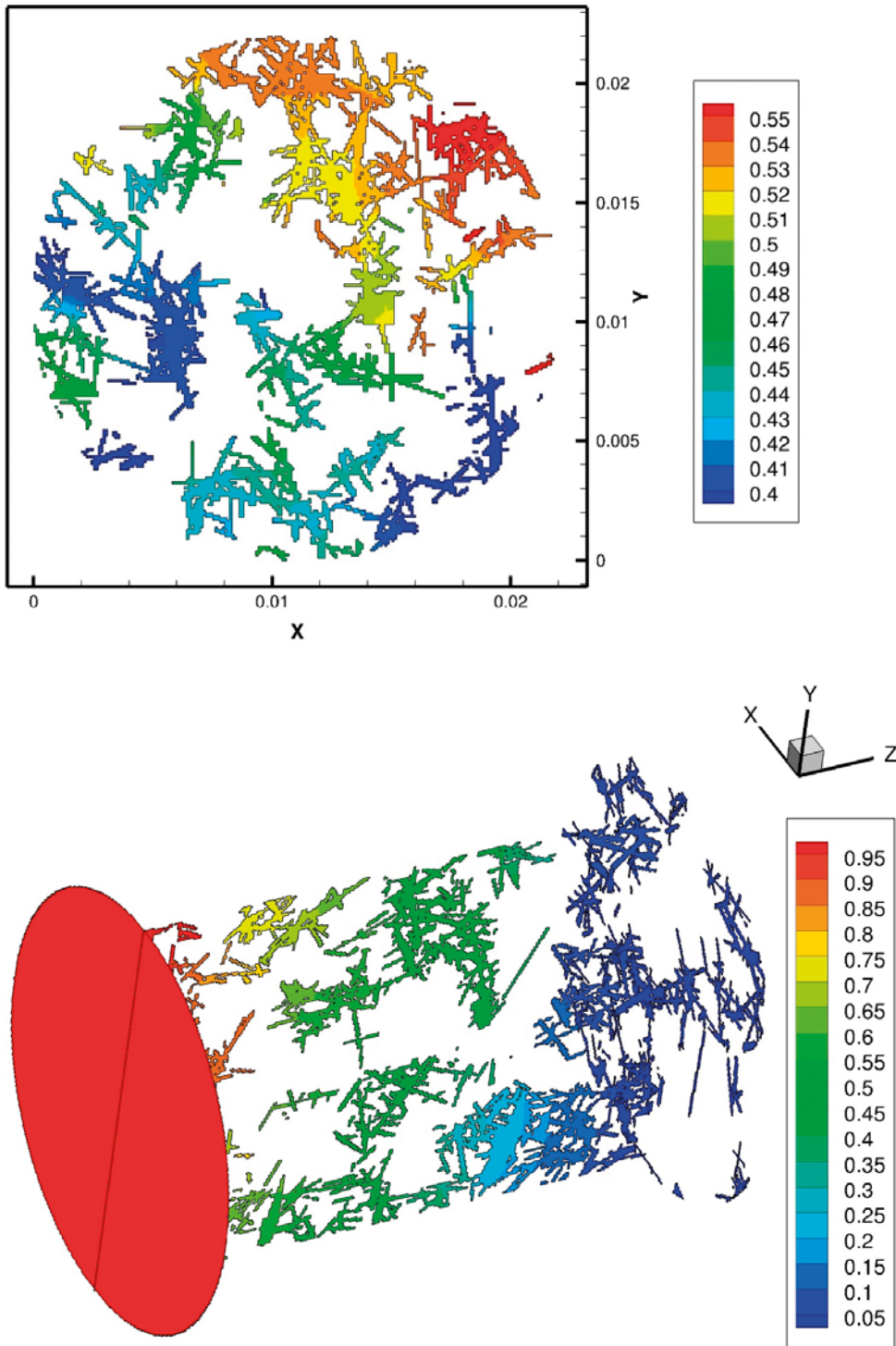


**Figure 3-8.** 3D Through-Diffusion. Tracer distribution in a section (top) and a perspective view. Coordinates in [m] (top figure).

### 3.4 LTDE, generic

Next we consider the case outlined in Figure 3-9, which is close to the “Target Fracture case” in LTDE (A-samples). The objective of this case is to illustrate the effect of “quartz veins”.

The following points give the details:

- On top a fracture with a cocktail of radionuclides is specified. Fracture aperture is set to 0.5 mm.
- The domain size is  $5 \times 1 \times 10$  cm.
- Grain size is 1.5 mm. Reactive grains represent about 6 % of the volume.
- The fracture at the low end  $x$ -coordinate is intended to represent a quartz vein. The aperture is set to 0.1 mm, the diffusivity to  $4 \times 10^{-10}$  m<sup>2</sup>/s and no reactive grains are specified for a distance of 1 mm from the fracture.
- Around 2000 particles are initially distributed in the target fracture. During the simulation, 3000 more are introduced (linear in time) in order to keep the concentration in the cocktail approximately constant.
- Integration time is 200 days.
- From the measurements the porosity is found to be around 0.2 % and increases to a few % towards the target fracture (Widstrand et al. 2010a, p 75). In the model the porosity is 0.24 % in the matrix and increases to 3 % close to the fracture.
- Four sorbing radionuclides are simulated. The  $K_d$  values, in brackets, are estimated from Table 4-11 in Widstrand et al. (2010a):  $Na-22(2 \times 10^{-4})$ ,  $Ni-63(3 \times 10^{-2})$ ,  $Cs-137(5 \times 10^{-2})$  and  $Co-57(10^{-1})$ .

The porosity distribution is given in Figure 3-10. This is also an illustration of the computational grid, as white areas give the areas where grid cells have been removed. White areas are hence grains. In Figure 3-11 red cells give the reacting grain boundary cells. It is thus in these cells a tracer may get sorbed.

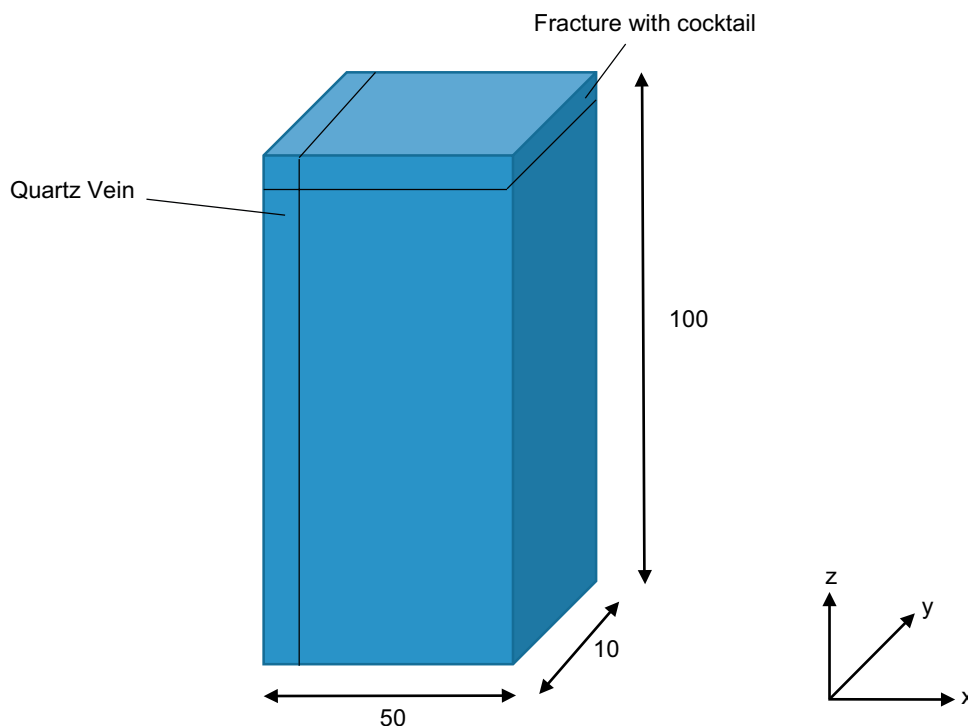


**Figure 3-9.** Generic LTDE case. Computational domain. Distances in [mm].



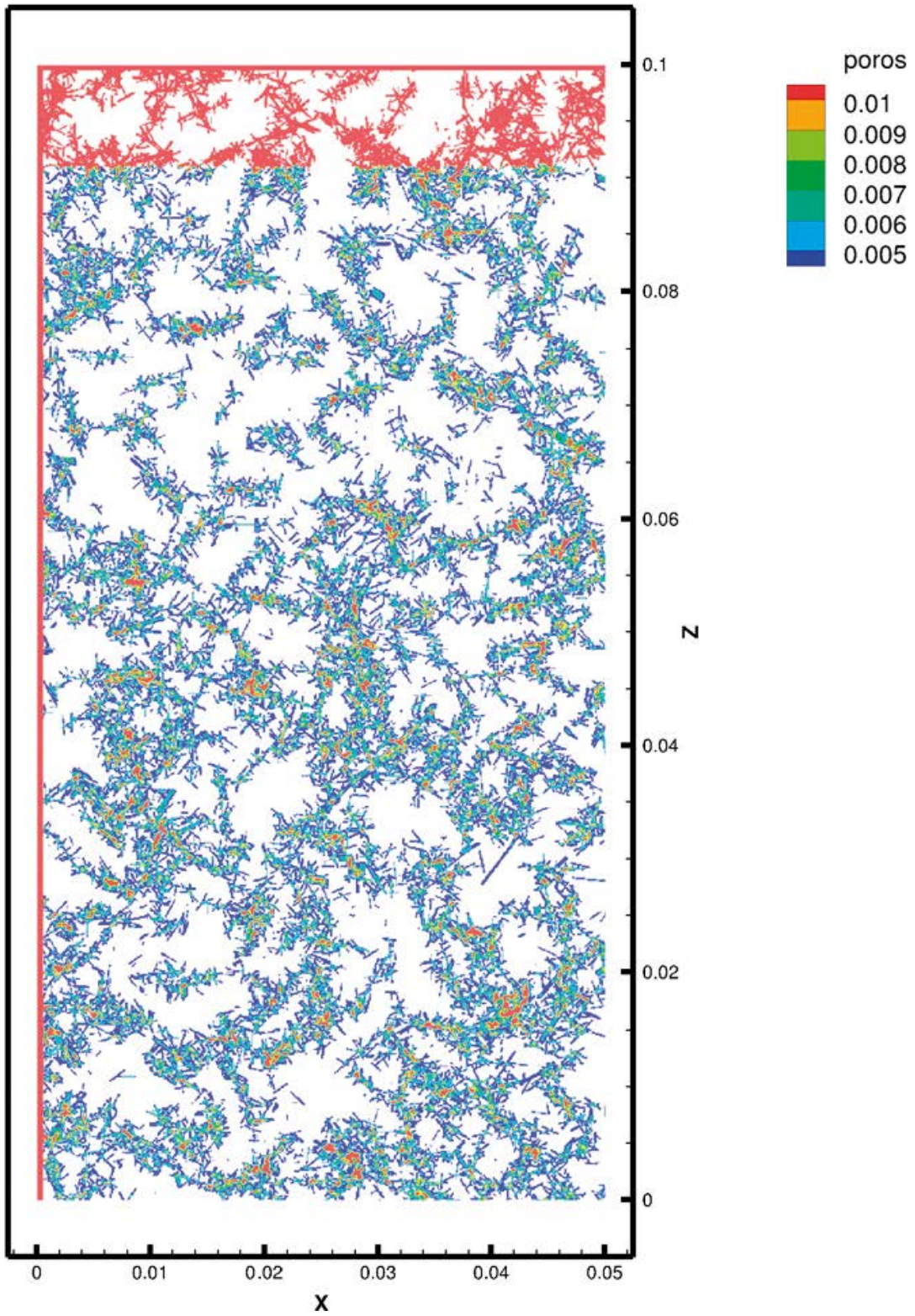


*Figure 3-10. Generic LTDE case. Porosity distribution in a section. Coordinates in [m].*

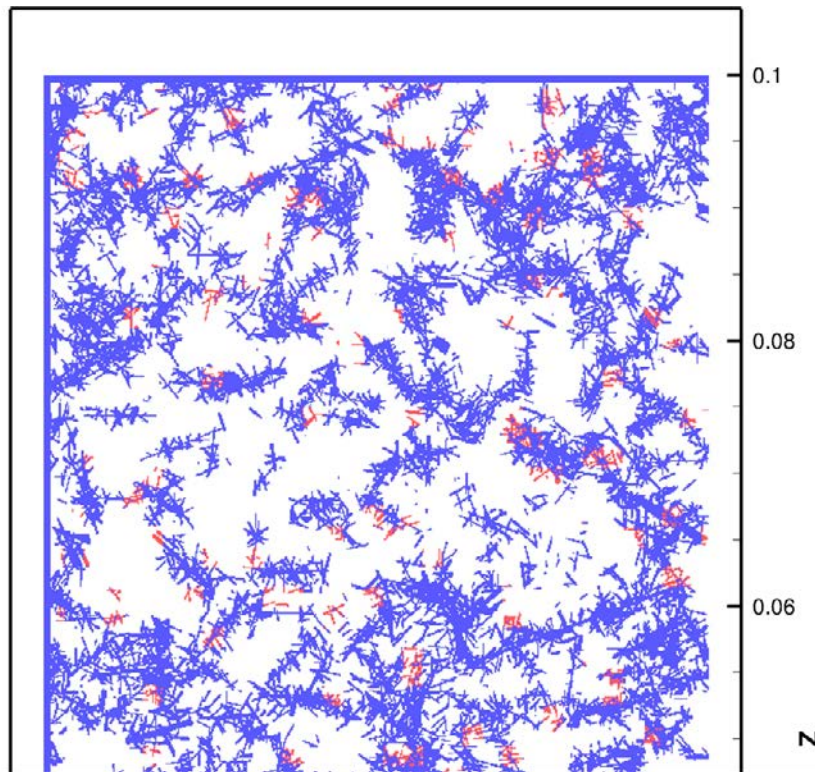


**Figure 3-11.** Generic LTDE case. Red cells give the reacting grain boundary cells. Coordinates in [m].

Particle distributions are shown for  $Na-22$  (least sorbing) in Figure 3-12 and for  $Co-57$  (most sorbing) in Figure 3-13. It is clear that the “quartz vein” contributes to the deep penetration. Concentration, in  $Bq/g$ , versus depth for the four tracers is shown in Figures 3-14 and 3-15. The curves are estimated by the postprocessor (Tecplot). It may be noted that for  $Na-22$  a straight line seems to fit equally well.

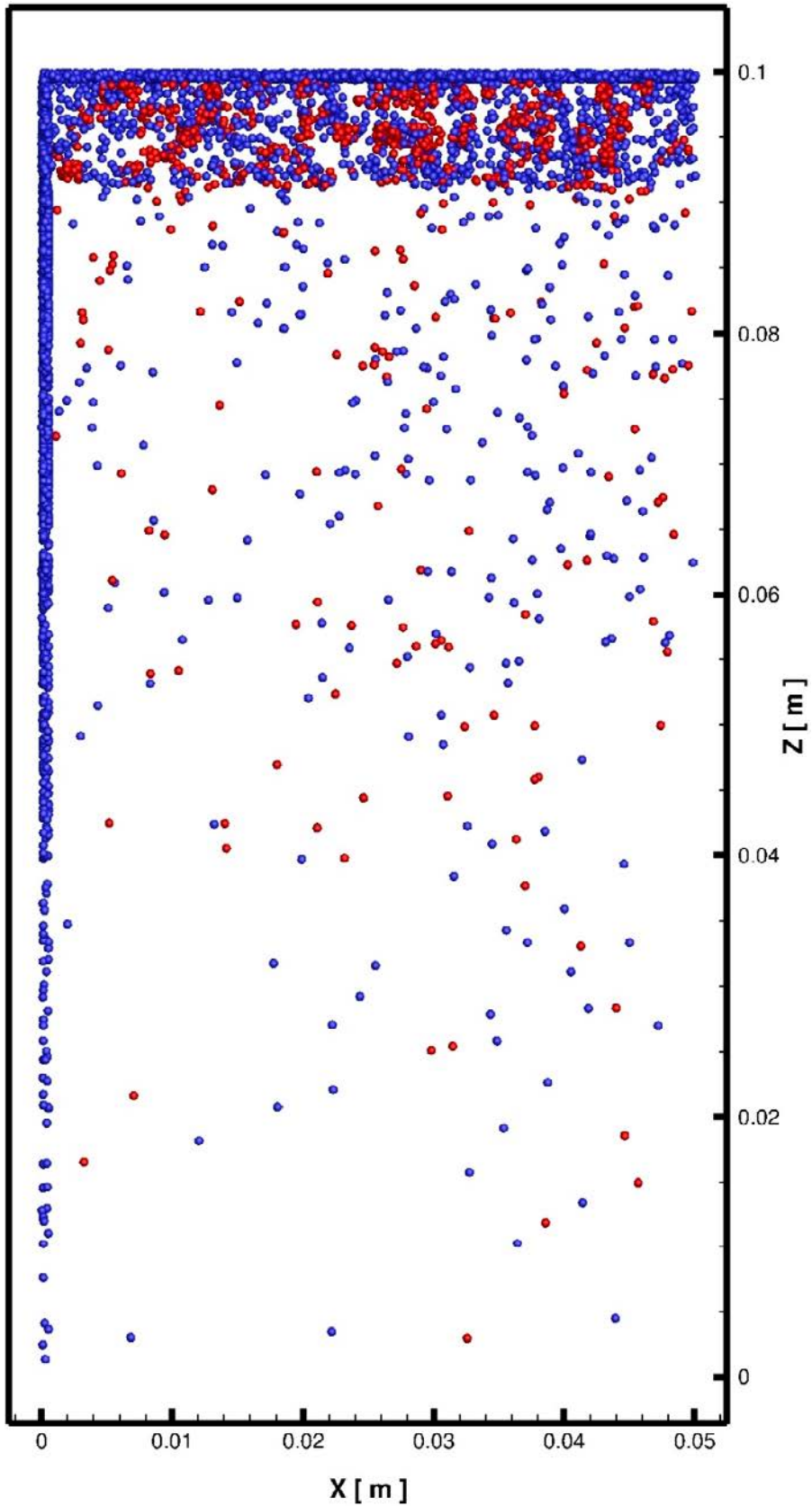


*Figure 3-12. Generic LTDE case. Particle distribution for Na-22 after 200 days of integration. Red particles are sorbed.*

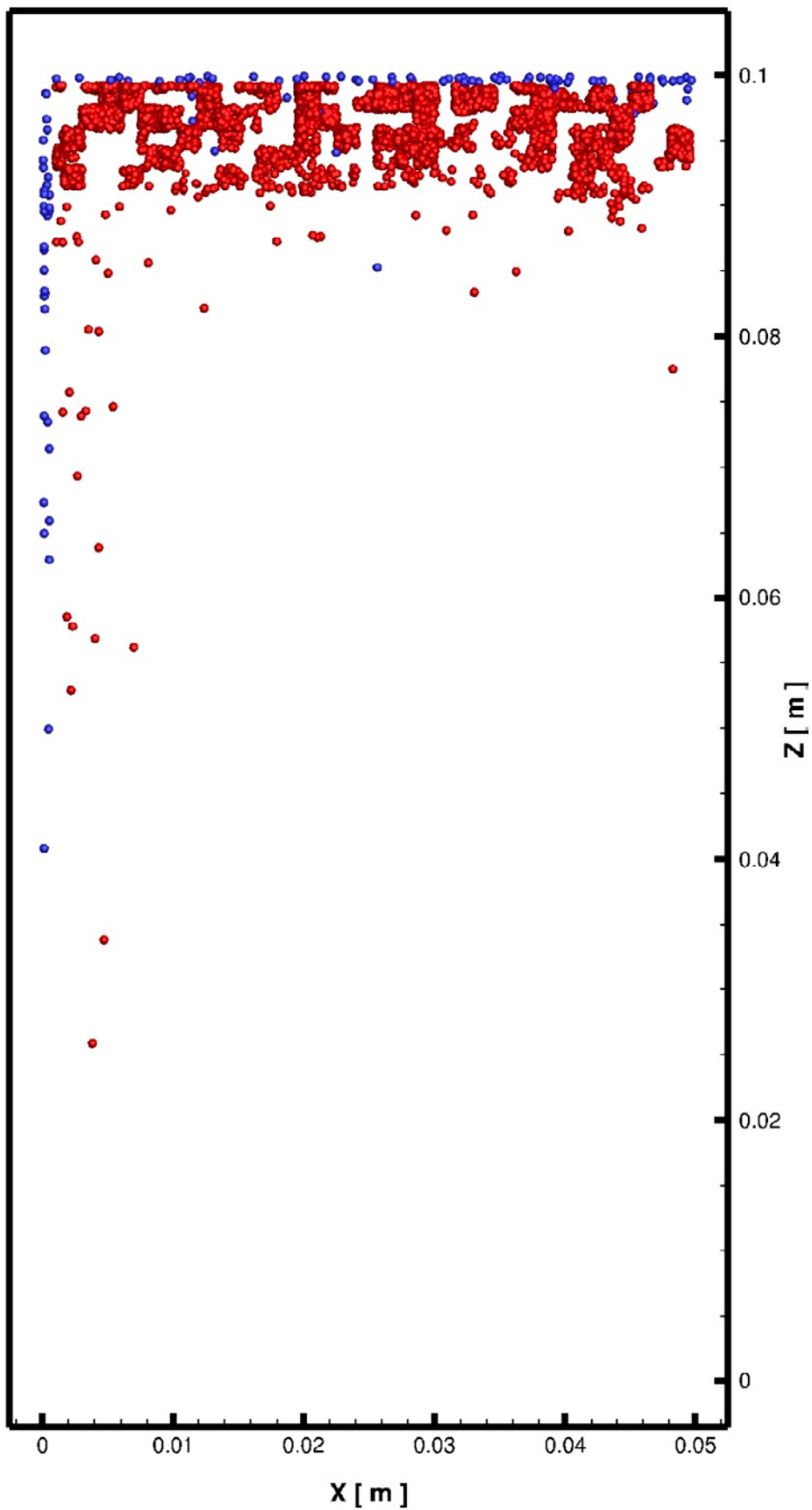


*Figure 3-13. Generic LTDE case. Particle distribution for Co-57 after 200 days of integration. Red particles are sorbed.*

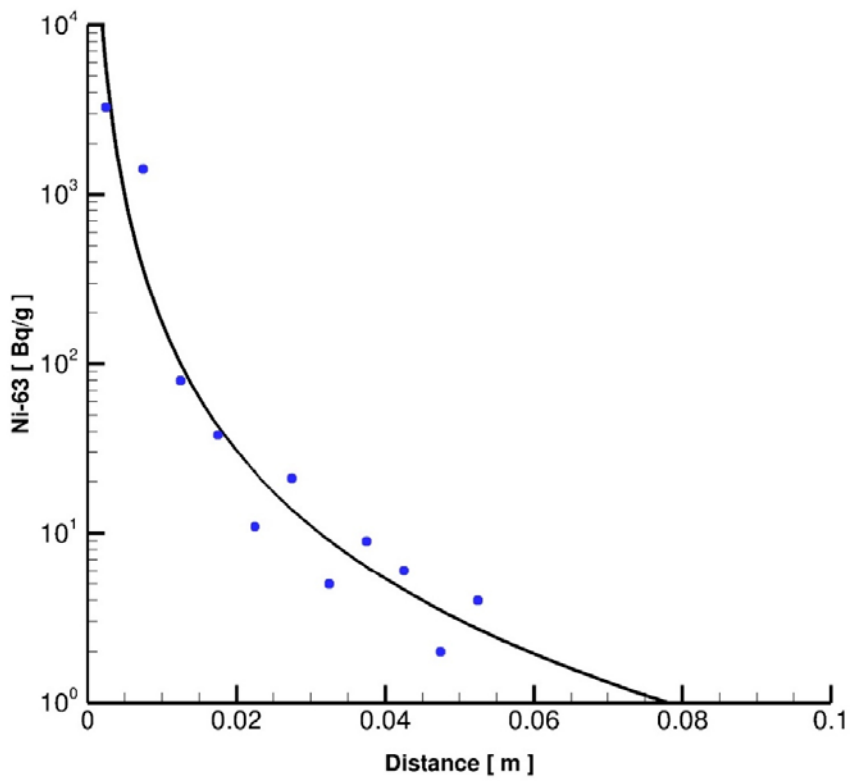
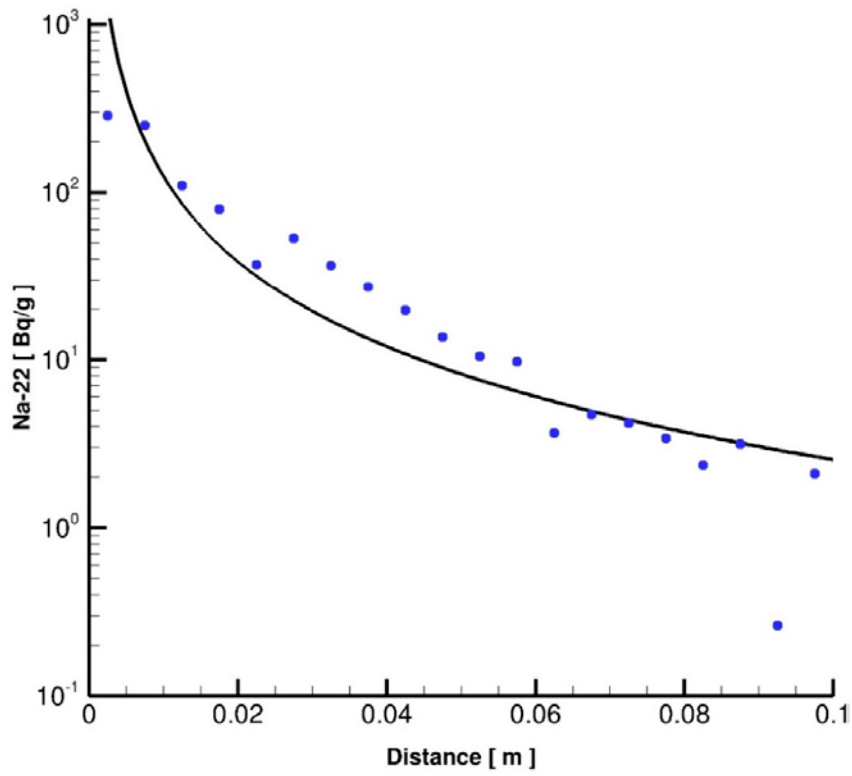


**Figure 3-14.** Generic LTDE case. Concentration versus depth for Na-22 (top) and Ni-63. Dots represent simulated data and curves are fitted to these.

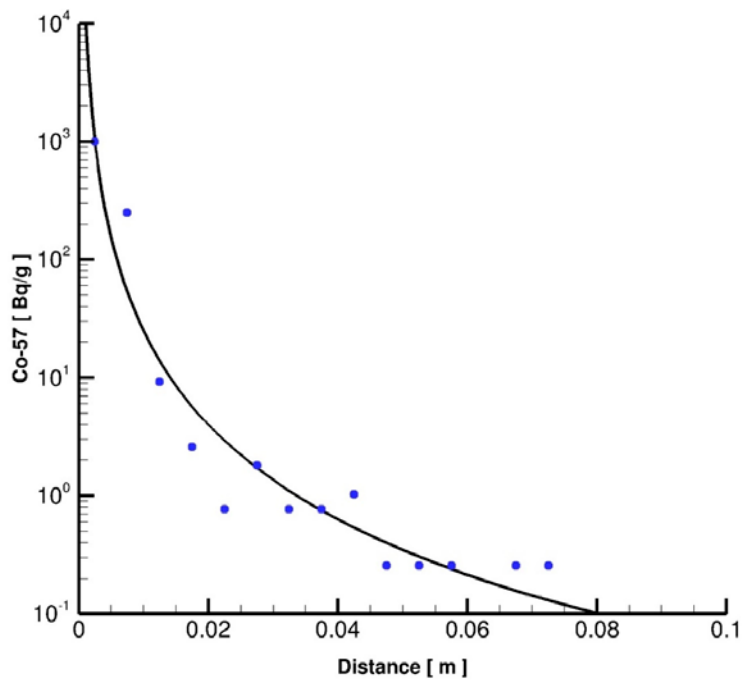
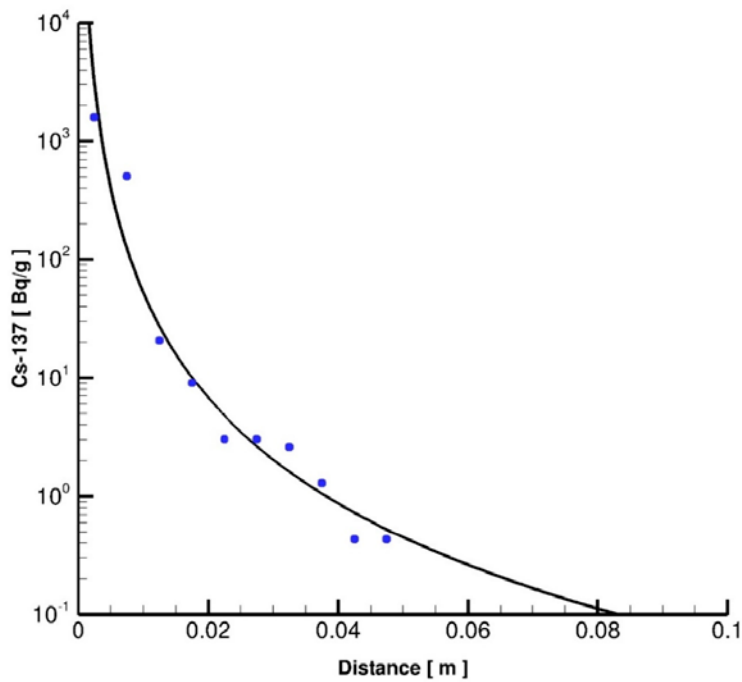


*Figure 3-15. Generic LTDE case. Concentration versus depth for Cs-137 (top) and Co-57. Dots represent simulated data and curves are fitted to these.*

### 3.5 LTDE, the stub

An outline of the stub, the A-cores and the deterministic fractures was given in Figure 2-5. This will be our computational domain, although somewhat smaller; the diameter was set to 0.14 m (instead of 0.177 m) and the length to 0.08 m. The only reason for this is to reduce the number of computational cells. A cell size of 0.2 mm was used and that resulted in a grid of about 88 million cells.

The grid is shown in Figure 3-16. The circular  $xy$  section is located about 10 mm from the target fracture; we will use this section in the following figures. In Figure 3-17 the porosity distribution is given. It is easy to identify the deterministic fractures. Cells that are in contact with a reacting grain are shown as red in Figure 3-18. It should be noted that no red cells are found in the deterministic fractures.

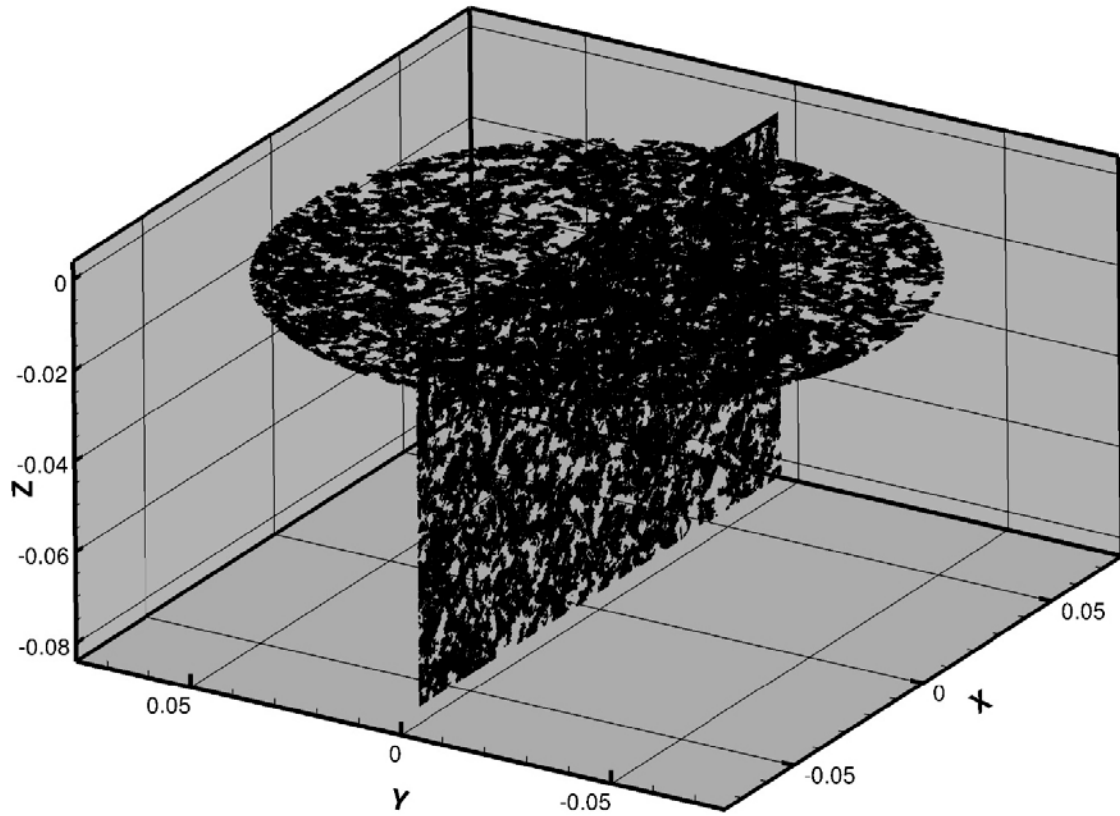


Figure 3-16. LTDE, the stub. Outline of domain and grid in two sections. Coordinates in [m].

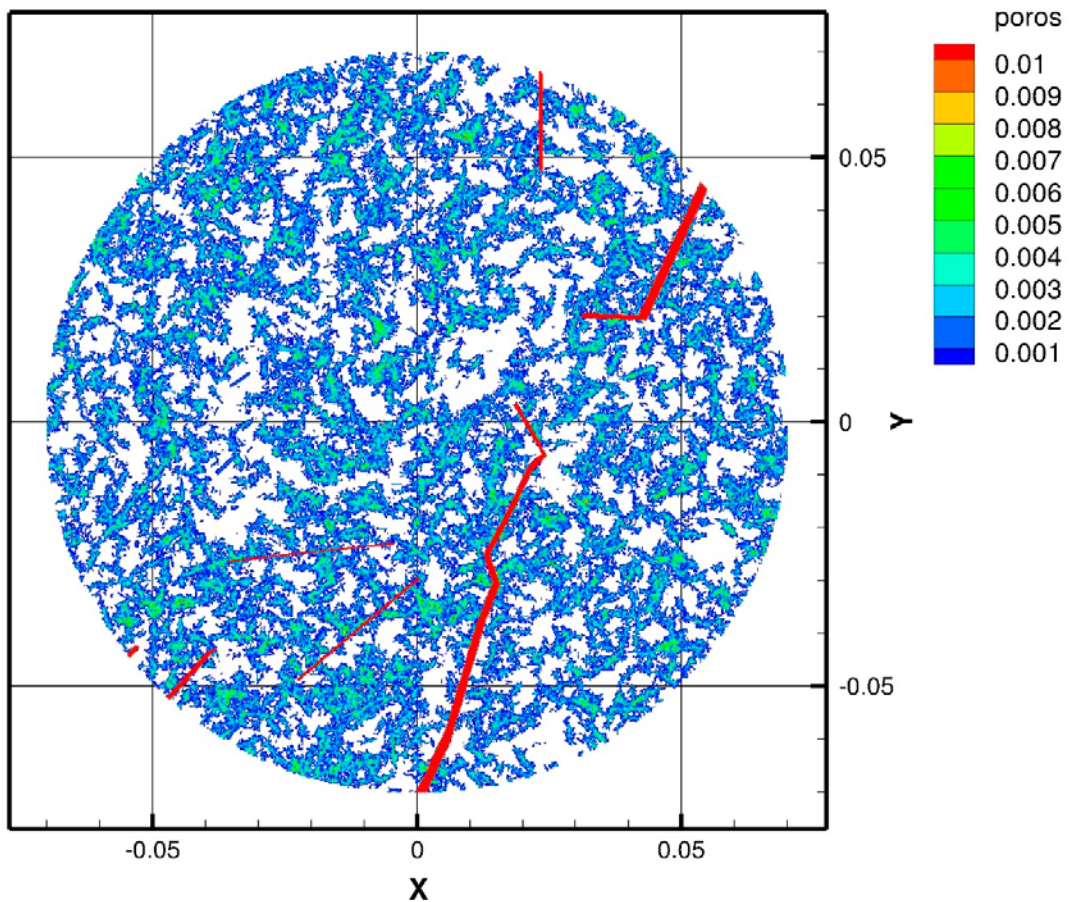
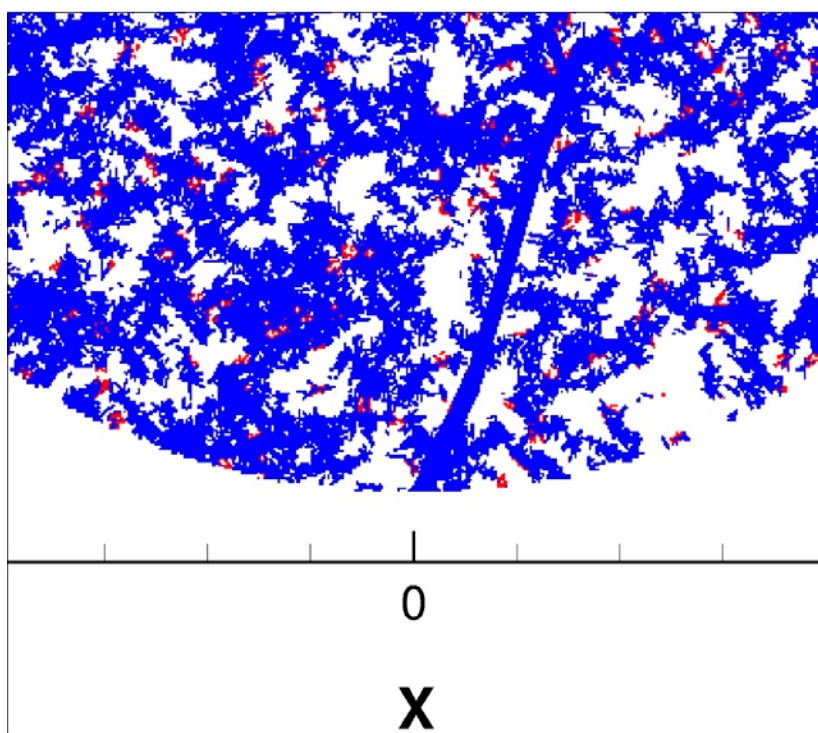
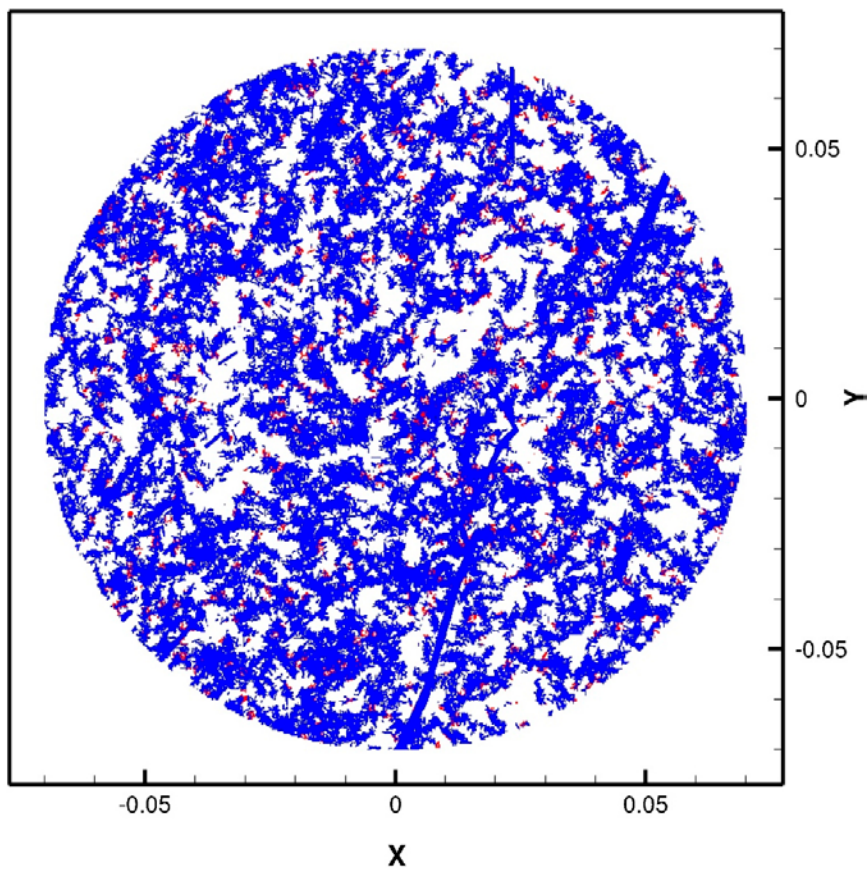


Figure 3-17. LTDE, the stub. Porosity distribution. Coordinates in [m].



**Figure 3-18.** LTDE, the stub. Red cells indicate the reacting grain boundary cells. Coordinates in [m].



We use the particle tracking method for the diffusion problem. In Figure 3-19 the distribution of a non-reacting tracer after 200 days of integration is shown. An increased density is found in the deterministic fractures. Particle distributions for  $Na-22$  and  $Ni-63$  are shown in Figures 3-20 and 3-21. The penetration depth is found to decrease with an increasing  $K_d$  value, as expected.

Finally, we show the penetration profiles for five tracers in Figures 3-22 and 3-23. For  $Cl-36$ , which does not sorb, it is expected that anion exclusion affects the process. This was accounted for by arbitrarily reducing the diffusion coefficients with a factor of 10. In Figure 3-22, the distribution with/without the reduction is shown.

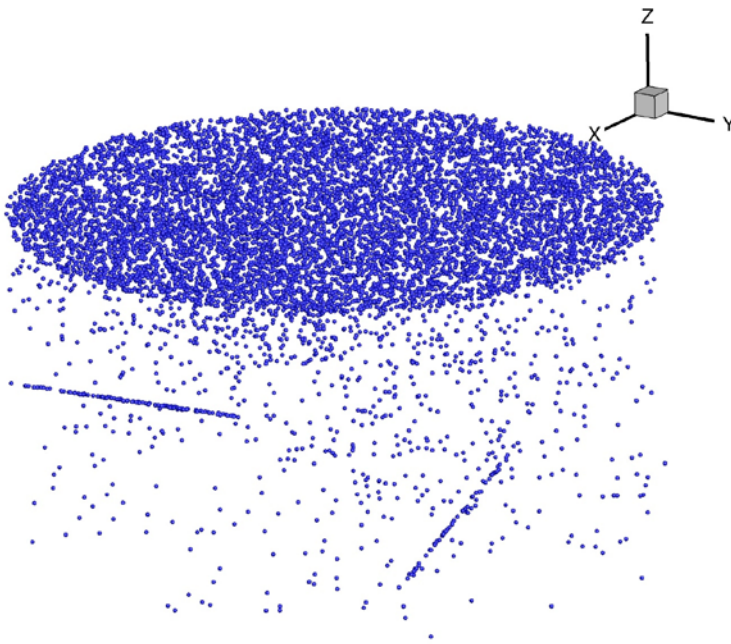


**Figure 3-19.** LTDE, the stub. Particle distribution for a non-reacting tracer after 200 days of integration.

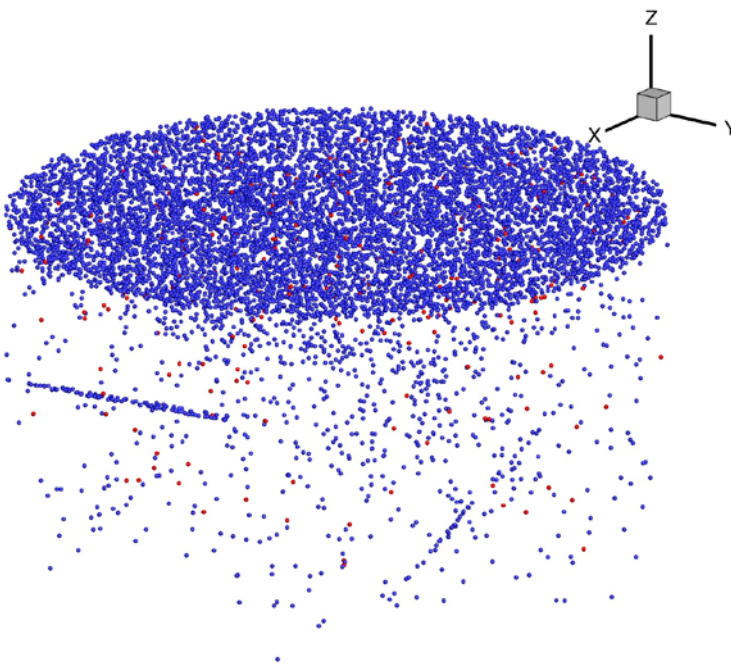


**Figure 3-20.** LTDE, the stub. Particle distribution for a tracer with  $K_d \approx 2 \times 10^{-4}$  ( $Na-22$ ) after 200 days of integration. Red particles are sorbed.

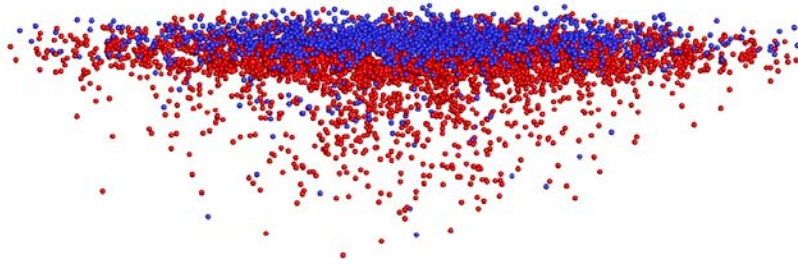
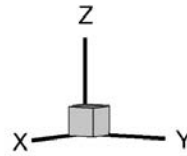


**Figure 3-21.** LTDE, the stub. Particle distribution for a tracer with  $K_d \approx 3 \times 10^{-2}$  (Ni-63) after 200 days of integration. Red particles are sorbed.

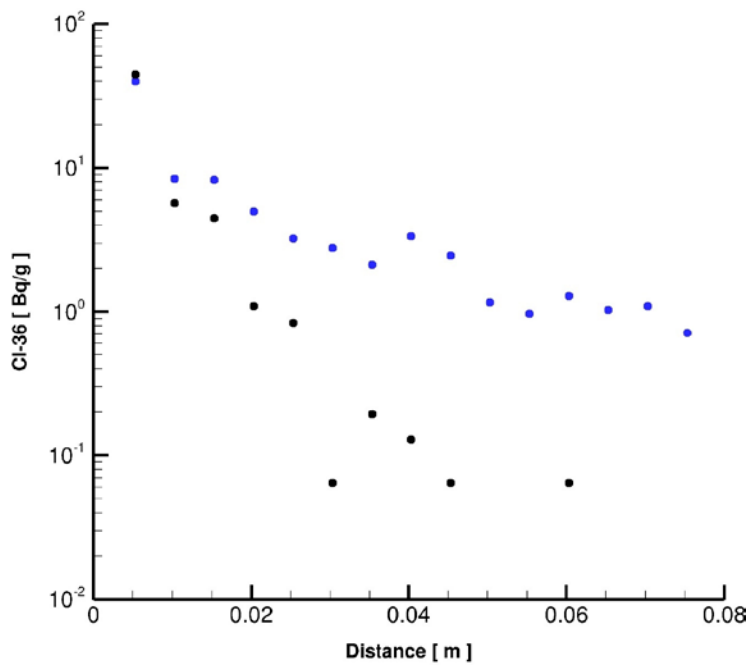
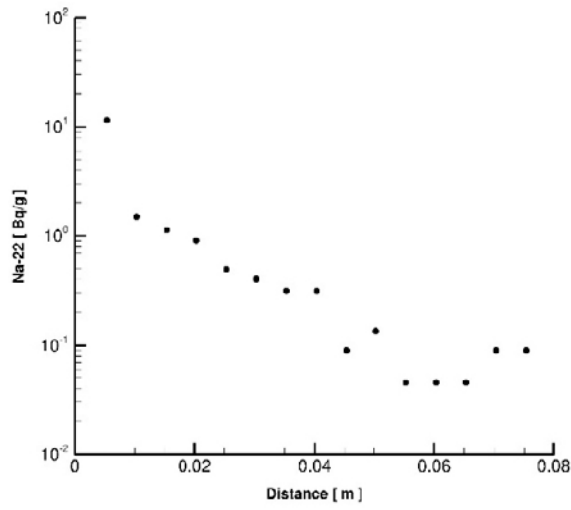
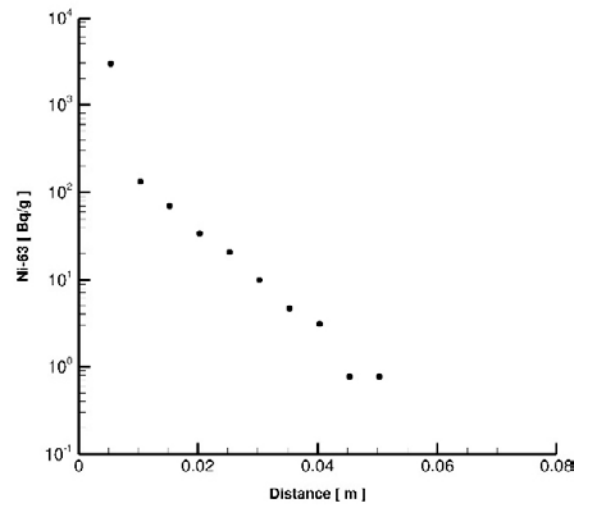


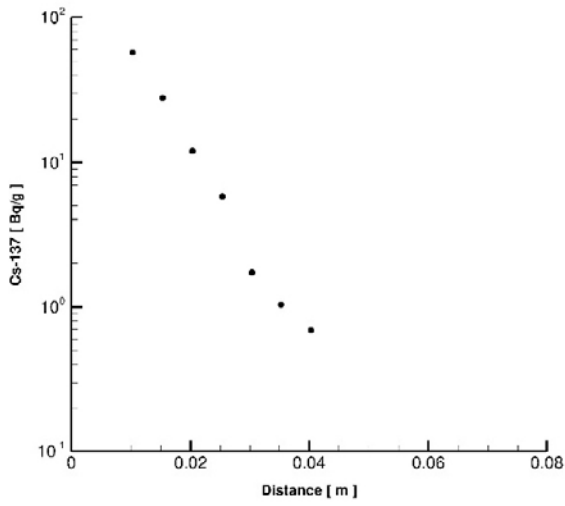
**Figure 3-22.** LTD, the stub. Concentration versus depth for Cl-36. Blue dots represent a simulation without reduction of the diffusion coefficient. Black dots represent a simulation where the diffusion coefficient was reduced with a factor of 10.



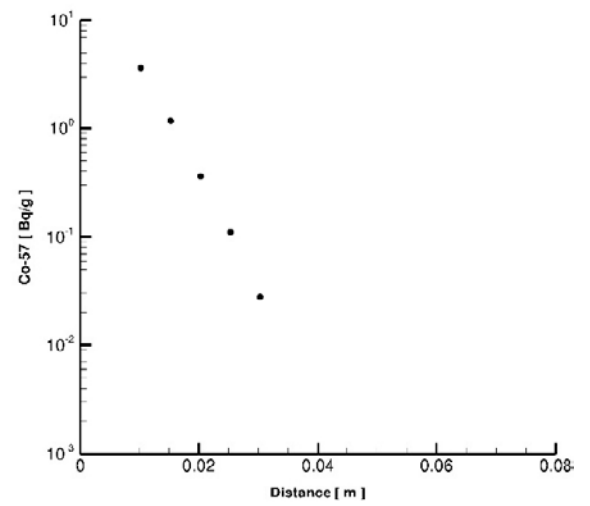
*Na-22*



*Ni-63*



*Cs-137*



*Co-57*

**Figure 3-23.** *LTDE, the stub. Concentration versus depth for four reacting tracers.*



## 4 Discussion

Grain scale reactive transport modelling is far from a standard method and it is thus relevant to discuss the accuracy, or the uncertainty, of the results presented. It is also relevant to discuss how accurate the experimental data are.

### 4.1 Experimental data

During Task 9B it has been discussed how accurate the measured profiles are. There are a number of concerns like: handling of samples after the experiment (after diffusion, evaporation), mass balances, deep penetration or contamination, etc. One may also question if it is relevant to analyze profiles from individual cores, as it assumes that the process is a 1D diffusion process. In this report, a 3D fracture network has been introduced; this network violates the 1D assumption.

### 4.2 Basic knowledge

Here we have made assumptions like “6 % reactive grains” and a  $K_d$  for each radionuclide. With the approach used in this report it is more relevant to ask how each radionuclide reacts with each mineral type. This is of course a hard question to answer as we need to consider tens of mineral types for each radionuclide. For accurate simulations it seems however that this information is needed.

### 4.3 The model

There are several aspects of the simulation model that create uncertainty. The grain block used is synthetic and should be replaced with data from X-ray tomography; this can be done. The altered zone is here treated as a region with higher fracture intensity; this in order to increase the porosity. It has been realized that the altered zone is very important for the penetration profiles and improvements of the description of the altered zone are called for. Once again X-ray data can help.



## 5 Summary and conclusions

The following points summarize the report:

- A synthetic grain block was developed. A certain percentage of the grains was prescribed as reactive. This was a useful step before X-ray micro computed tomography data was introduced.
- A reactive transport model based on particle tracking was introduced. Based on the concept “when a particle is close to a reactive grain it has a certain probability to get sorbed during a certain time span. Once sorbed it will stay so a certain time”, this model has proved to be a useful tool.
- Quartz veins. The experimental data suggested “deep penetration into the rock matrix”. One way to achieve this in the models is to introduce deterministic fractures and assume that these go through quartz grains (quartz grains are not reactive). Experimental data for the fractures were available.
- Computational methods. A grid that resolved the intergranular space was developed; cells inside grains could be removed, which reduced the number of cells significantly. For particle tracking the CTRW (Continuous Time Random Walk) method was included as an option in DarcyTools.
- The model is used to simulate the LTDE-SD experiment.

The main conclusions to be drawn relate to the reactive particle tracking method developed in the project. In the report the parameters of the method are related to more traditional retention parameters, which is needed. However, the most important aspect is perhaps that each radionuclide considers reaction with each grain type present. This detailed resolution requires a computational grid that describes the intergranular space.





## References

SKB's (Svensk Kärnbränslehantering AB) publications can be found at [www.skb.com/publications](http://www.skb.com/publications).

**Crank J, 1975.** The mathematics of diffusion. 2nd ed. London Oxford University Press.

**Löfgren M, Nilsson K, 2020.** Task description of Task 9B – Modelling of LTDE-SD performed at Äspö HRL. Task 9 of SKB Task Force GWFTS – Increasing the realism in solute transport modelling based on the field experiments REPRO and LTDE-SD. SKB P-17-30, Svensk Kärnbränslehantering AB.

**Nilsson K, Byegård J, Selnert E, Widestrand H, Höglund S, Gustafsson E, 2010.** Äspö Hard Rock Laboratory Long Term Sorption Diffusion Experiment (LTDE-SD) Results from rock sample analyses and modelling. SKB R-10-68, Svensk Kärnbränslehantering AB.

**Russian A, Dentz M, Guoze P, 2016.** Time domain random walks for hydrodynamic transport in heterogeneous media. *Water Resources Research* 52, 3309–3323

**Svensson U, Ferry M, 2014.** DarcyTools: a computer code for hydrogeological analysis of nuclear waste repositories in fractured rock. *Journal of Applied Mathematics and Physics* 2. doi:10.4236/jamp.2014.26044

**Svensson U, Löfgren M, Trincherio P, Selroos J-O, 2018.** Modelling the diffusion-available pore space of an unaltered granitic rock matrix using a micro-DFN approach. *Journal of Hydrology* 559, 182–191.

**Svensson U, Voutilainen M, Muuri E, Ferry M, Gylling B, 2019a.** Modelling transport of reactive tracers in a heterogeneous crystalline rock matrix. *Journal of Contaminant Hydrology* 227. doi:10.1016/j.jconhyd.2019.103552

**Svensson U, Trincherio P, Ferry M, Voutilainen M, Gylling B, Selroos J-O, 2019b.** Grains, grids and mineral surfaces: approaches to grain scale matrix modelling based on X-ray micro-computed tomography data. *SN Applied Sciences* 1, 1277. doi:10.1007/s42452-019-1254-1

**Widestrand H, Byegård J, Selnert E, Skålberg M, Höglund S, Gustafsson E, 2010a.** Long Term Sorption Diffusion Experiment (LTDE-SD) Supporting laboratory program – Sorption diffusion experiments and rock material characterisation With supplement of adsorption studies on intact rock samples from the Forsmark and Laxemar site investigations. SKB R-10-66, Svensk Kärnbränslehantering AB.

**Widestrand H, Byegård J, Nilsson K, Höglund S, Gustafsson E, Kronberg M, 2010b.** Long Term Sorption Diffusion Experiment (LTDE-SD) Performance of main in situ experiment and results from water phase measurements. SKB R-10-67, Svensk Kärnbränslehantering AB.

SKB is responsible for managing spent nuclear fuel and radioactive waste produced by the Swedish nuclear power plants such that man and the environment are protected in the near and distant future.

**skb.se**